Universal Journal of Aeronautical & Aerospace Sciences **2 (2014), 55-79**
www.papersciences.com

Dynamic Behaviour of a Rocket Filled with Liquid

Y. Kerboua[*], A.A. Lakis[**]
[*]Mechanical Engineering Department, Constantine University 1, Algeria
B.P. 325 Route Ain El Bey, Constantine 25017, Algeria
[**]Mechanical Engineering Department, École Polytechnique of Montréal, Canada
C.P. 6079, Succursale Centre-ville, Montréal, Québec, Canada H3C 3A7
aouni.lakis@polymtl.ca

Abstract
The purpose of this paper is to present a numerical model able to simulate the dynamic behaviour of a rocket structure coupled with fluid. To provide perfect geometrical consistency, two semi-analytical finite elements (conical and cylindrical) are combined to model the fluid-structure interaction problem. The displacement functions of each finite element are obtained from exact solutions of the corresponding Sanders shell equilibrium equations. The fluid pressure applied on the wall of the structure is derived from the velocity potential, Bernoulli equation and from the impermeability condition applied to ensure permanent coupling at the fluid-solid interface. The fluid pressure and the mass and stiffness of each finite element are determined by exact analytical integration to establish the dynamic equations of the fluid-shell. The results obtained compare well with those of experimental and numerical studies available in literature.

Keyword and Phrases
Fluid-Structure Interaction, Vibrations, Combined Shell, Finite Elements, Rocket.

1. Introduction

Many structural elements that consist of axisymmetric shells in contact with fluid are found in various fields of engineering such as aircraft fuselages, elevated tanks in civil engineering, pipes and pressure vessels, the components of nuclear power plants, rocket construction and components of submarine industry. The fluid influences the dynamic behaviour of the structure in many ways depending on whether it is at rest or flowing. Precise knowledge of the dynamic behaviour of shells influenced by interior/exterior fluid is therefore of considerable interest.

The fluid-structure interaction of cylindrical shells has attracted the attention of many researchers, starting with the early works of Rayleigh [20] and Lamb [19] which constitute the basic theory of the behaviour of the internal fluid. A wide choice of literature is available. Berry and Reissner [15] did a theoretical study of the behaviour of a pressurized cylindrical shell completely filled with heavy fluid. Lindholm et al. [23] experimentally studied the vibrations of a fully and partially filled cylindrical shell. Coale and Nagano [24] calculated the axisymmetric frequencies of a liquid-filled cylindrical shell joined to a hemispherical shell. Lakis and Païdoussis developed a semi-analytical finite element to analyze the dynamic behaviour of cylindrical shells based on classical shell theory and the finite element method [18]. This model has been successfully extended to study the dynamic behaviour of a shell subjected to: potential flow [10], the turbulent boundary layer of an internally flowing fluid [25] and supersonic flow [26]. Several other interesting works have been performed to study various aspects of the dynamic behaviour of a cylindrical shell coupled with fluid ([27] to [29]).

The dynamic behaviour of conical shells in contact with fluid has not been as extensively studied as the case of cylindrical shells. Ross and Seers [30] carried out experimental and numerical investigations on the non-linear vibration of conical shells subjected to external water pressure. The finite element method was applied to build a theoretical model of the fluid and solid. Nishimura and Shingu [31] studied the dynamic behaviour of submerged conical shells. A

combination of the finite element method and Fourier series has been used to model the fluid-structure interaction problem. Sweedan & A. A. El Damatty [32] conducted an experimental study to evaluate the dynamic characteristics of a liquid-filled conical shell. The results were compared to those obtained using their previously-developed numerical model in references [33] and [34]. Lakis et al. [8] carried out a dynamic analysis of anisotropic fluid-filled truncated conical shells. The same formulation has been applied to predict the dynamic behaviour of anisotropic truncated conical shells conveying fluid [6] and [36]. Conical shell subjected to flowing fluid has also been investigated by Senthil-Kumar and Ganesan [35]. The solid shell was formulated using a semi-analytical finite element based on first-order shear deformation theory. The fluid domain has been modelled using an annular semi-analytical ring element. Liu et al. [37] presented an analytical method to predict the vibration of ring-stiffened conical shells with variable thickness under fluid loading. The fluid loading was taken into account by dividing the shell into narrow strips which were considered to be locally cylindrical. The governing equations of vibration of a ring-stiffened conical shell were developed based on Flügge theory and the equivalent method of ring-stiffeners. Caresta and Kessissoglou [38] presented an analytical solution to calculate the low frequency of conical shells with fluid loading. The power series solution method for different boundary conditions was applied based on a local cylindrical approximation of a conical shell.

Much less interest has been given to study the dynamic behaviour of combined conical-cylindrical shells coupled with fluid. This is mainly due to difficulties coupling the solid and fluid equations associated with two different geometries; conical and cylindrical. This class of structures is found in many important industrial applications such as aeronautical, aerospace and civil industries. Torpedo-shaped structures such as rockets, submarines, elevated liquid tanks and aircraft fuselages are examples. Unfortunately, all of the investigations cited above were limited to either conical or cylindrical shells coupled with the fluid. Only a few research efforts related to this specific case combining these two shapes have been carried out. El-Damatty et al. [3] conducted an experimental study on a small-scale combined liquid-filled conical shell model. The fundamental frequencies of vibration and the associated $\cos(\theta)$ modes were determined. Experimental results were compared with previously-developed numerical data in reference [33]. Pun et al. [39] carried out an experimental study on underwater vibration of a torpedo-shaped structure. The structure comprises three parts of axisymmetrical shells, hemispherical, cylindrical and conical, joined together. The possibility to link the wet and dry modes of the underwater structure was investigated.

This work arises as part of a research project on the vibration of a rocket structure coupled with the surrounding flowing fluid. The purpose of the present paper is to predict the dynamic behaviour of a combined conical-cylindrical shell coupled with internal fluid. First it is ascertained that the geometric transformations and the combined conical-cylindrical shell without fluid is correctly represented. Thereafter, a validation of fluid-structure coupling techniques is carried out in the context of the present work. A combination of two semi-analytical conical and cylindrical finite elements is used. The advantage in using both of these finite elements lies in the fact that their displacement functions can be obtained by exact solutions of the corresponding Sanders shell equilibrium equations. The velocity potential, Bernoulli equation and the impermeability condition are used to calculate the fluid pressure applied on the shell wall.

2. Modeling of Combined Conical-Cylindrical Shells in a Vacuum

To accurately predict the dynamic behaviour of a rocket made of combined conical-cylindrical shells as shown in Figure 1, two axisymmetric finite elements are adopted. The middle surface of each element is matched with the middle surface of the axisymmetric shell. The equations of motion of cylindrical and conical shells are derived from Sanders' thin shell theory [14]. The latter is based on Love's first approximation and results in zero strain values for small rigid-body motion. This is more advantageous than other existing theories [18] (Reissner [15], Vlasov [16] and Timoshenko [17]).

Both conical and cylindrical finite elements use complete thin shell equations for determination of the displacement functions, and consequently the elementary matrices of mass and stiffness. This provides a much more precise method than obtained using polynomial displacement functions as is typically the case in finite element methods [18].

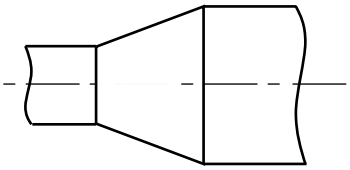

Fig. 1 Combined conical-cylindrical shell

Unlike the ordinary finite element method, this approach can be easily adapted to take into account the hydrodynamic effects induced by fluid structure interaction, because of its use of classical theory for the displacement functions. Moreover, high as well as low frequencies can be obtained with high accuracy [18]. This is useful for free vibration analysis but is also of considerable importance in determining the response of such shells to random pressure fields, such as pressure fields generated by internal or external flow.

This approach was used successfully by our research group to develop semi-analytical models to analyze separately the vibration of conical and cylindrical shells in a vacuum and/or when coupled with fluid. The basic model [18] was developed to obtain the free vibration characteristics of the cylindrical shell without fluid. This model was adapted to predict the dynamic behaviour of a cylindrical shell filled with liquid by taking into consideration the free surface effect [9]. Based on the same approach, Lakis et al. carried out analysis of the case of cylindrical shells and conical shells subjected to potential flow, see references [1], [38][6], [8]. The case of cylindrical shells subjected to a random pressure field arising from an internal flow boundary was conducted by Lakis and Païdoussis in reference [24]. Aeroelastic analysis of cylindrical and conical shells subjected to supersonic airflow was conducted in references [25] and [35], respectively, using the same semi-analytical method. This approach combines the advantages of finite element method and the precise formulation of classical shell theory.

2.1. Cylindrical Shell Model

The cylindrical part of the combined shell is modeled using a cylindrical panel segment defined by two line-nodes, i and j. Each node has four degrees of freedom: three displacements (axial, circumferential and radial) and one rotation oriented as shown in Figure 2. The equilibrium equations of a cylindrical shell are employed to obtain the pertinent displacement functions instead of using polynomial functions. This approach has given very accurate results [18] using a small number of finite elements.

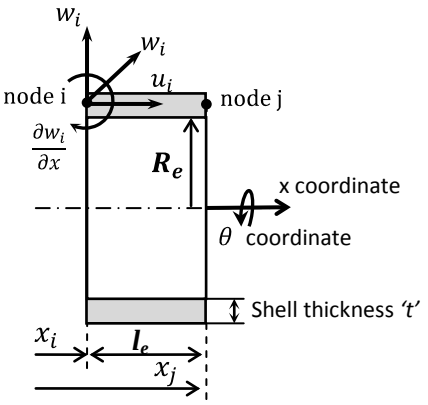

Fig. 2 Geometry and nodal displacements of the cylindrical finite element

2.1.1. Equations of Motion

The equilibrium differential equations for cylindrical shells in terms of axial, circumferential and radial displacement are given bellow [18]:

$$L_1(U,V,W,P_{ij}) = 0 \tag{2.1.1.a}$$

$$L_2(U,V,W,P_{ij}) = 0 \tag{2.1.1.b}$$

$$L_3(U,V,W,P_{ij}) = 0 \tag{2.1.1.c}$$

where L_k (k = 1, 2, 3) are three linear differential operators, the form of which is given fully in Appendix A. P_{ij} terms are the components of an anisotropic matrix of elasticity [P] of order (6×6), see Equation 14 below.

2.1.2.Displacement Functions

The displacement field is defined for the n^{th} wave number by the following expressions:

$$\begin{Bmatrix} U(x,\theta) \\ W(x,\theta) \\ V(x,\theta) \end{Bmatrix} = \begin{bmatrix} \cos(n\theta) & 0 & 0 \\ 0 & \cos(n\theta) & 0 \\ 0 & 0 & \sin(n\theta) \end{bmatrix} \begin{Bmatrix} u(x) \\ w(x) \\ v(x) \end{Bmatrix} = [T_n] \begin{Bmatrix} u(x) \\ w(x) \\ v(x) \end{Bmatrix} \tag{2.1.2.1}$$

The displacements in axial direction are represented by the following functions (see reference [18]):

$$\begin{Bmatrix} u(x) \\ w(x) \\ v(x) \end{Bmatrix} = \begin{Bmatrix} A.e^{\left(\frac{\lambda.x}{L_e}\right)} \\ B.e^{\left(\frac{\lambda.x}{L_e}\right)} \\ C.e^{\left(\frac{\lambda.x}{L_e}\right)} \end{Bmatrix} \tag{2.1.2.2}$$

where: A, B, C and λ are complex numbers. l_e is the finite element length in the axial direction (x). Replacing $U(x,\theta), V(x,\theta)$ and $W(x,\theta)$ in the equilibrium equations, we obtain the following system:

$$\begin{bmatrix} H_{11} & H_{12} & H_{13} \\ H_{21} & H_{22} & H_{23} \\ H_{31} & H_{32} & H_{33} \end{bmatrix} \begin{Bmatrix} A \\ B \\ C \end{Bmatrix} = \begin{Bmatrix} 0 \\ 0 \\ 0 \end{Bmatrix} \tag{2.1.2.3}$$

Expressions of matrix $[H_{ij}]$ are provided in Appendix A. For non-trivial solutions the determinant of $[H_{ij}]$ must be equal to zero. This yields the following characteristic equation:

$$a\lambda^8 + b\lambda^6 + c\lambda^4 + d\lambda^2 + e = 0 \tag{2.1.2.4}$$

where:

a, *b*, *c*, *d* and *e* are coefficients of the characteristic equation depending on material properties, geometry and the circumferential mode n. Their mathematical expressions are given in reference [18]. Each root λ_j yields a solution of the equilibrium equation. The complete solution is the sum of the eight solutions. The displacement field may then be written as follows:

$$\begin{Bmatrix} U(x,\theta) \\ W(x,\theta) \\ V(x,\theta) \end{Bmatrix} = [T_n] \sum_{j=1}^{j=8} \begin{bmatrix} e^{\left(\frac{\lambda_j.x}{L_e}\right)} & 0 & 0 \\ 0 & e^{\left(\frac{\lambda_j.x}{L_e}\right)} & 0 \\ 0 & 0 & e^{\left(\frac{\lambda_j.x}{L_e}\right)} \end{bmatrix} \begin{Bmatrix} A_j \\ B_j \\ C_j \end{Bmatrix} \tag{2.1.2.5}$$

The complete solution is obtained by the sum of all eight including constants A_j, B_j and C_j. As these last constants are not independent, we may write $A_j = \alpha_j C_j$ and $B_j = \beta_j C_j$. Where: α_j and β_j are complex numbers given in reference [18]. The equation above may be written as follows:

$$\begin{Bmatrix} U(x,\theta) \\ W(x,\theta) \\ V(x,\theta) \end{Bmatrix} = [T_n][R]\{C\} \tag{2.1.2.6}$$

where the $[R]$ matrix and $\{C\}$ vector are expressed by:

$$[R] = \begin{bmatrix} \alpha_1 e^{\left(\frac{\lambda_1 x}{L_e}\right)} & \alpha_2 e^{\left(\frac{\lambda_2 x}{L_e}\right)} & \alpha_3 e^{\left(\frac{\lambda_3 x}{L_e}\right)} & \alpha_4 e^{\left(\frac{\lambda_4 x}{L_e}\right)} & \alpha_5 e^{\left(\frac{\lambda_5 x}{L_e}\right)} & \alpha_6 e^{\left(\frac{\lambda_6 x}{L_e}\right)} & \alpha_7 e^{\left(\frac{\lambda_7 x}{L_e}\right)} & \alpha_8 e^{\left(\frac{\lambda_8 x}{L_e}\right)} \\ e^{\left(\frac{\lambda_1 x}{L_e}\right)} & e^{\left(\frac{\lambda_2 x}{L_e}\right)} & e^{\left(\frac{\lambda_3 x}{L_e}\right)} & e^{\left(\frac{\lambda_4 x}{L_e}\right)} & e^{\left(\frac{\lambda_5 x}{L_e}\right)} & e^{\left(\frac{\lambda_6 x}{L_e}\right)} & e^{\left(\frac{\lambda_7 x}{L_e}\right)} & e^{\left(\frac{\lambda_8 x}{L_e}\right)} \\ \beta_1 e^{\left(\frac{\lambda_1 x}{L_e}\right)} & \beta_2 e^{\left(\frac{\lambda_2 x}{L_e}\right)} & \beta_3 e^{\left(\frac{\lambda_3 x}{L_e}\right)} & \beta_4 e^{\left(\frac{\lambda_4 x}{L_e}\right)} & \beta_5 e^{\left(\frac{\lambda_5 x}{L_e}\right)} & \beta_6 e^{\left(\frac{\lambda_6 x}{L_e}\right)} & \beta_7 e^{\left(\frac{\lambda_7 x}{L_e}\right)} & \beta_8 e^{\left(\frac{\lambda_8 x}{L_e}\right)} \end{bmatrix}$$

And

$$\{C\} = \{C_1 \quad C_2 \quad C_3 \quad C_4 \quad C_5 \quad C_6 \quad C_7 \quad C_8\}^T$$

The constants C_j (j=1, 8) may be replaced by the finite element nodal displacements vector $\{\delta\}^e$ using the eight boundary conditions of each finite element, four at each node as follows:

$$\{\delta\}^e = \left\{u_i, \quad w_i, \quad \frac{\partial w_i}{\partial x}, \quad v_i, \quad u_j, \quad w_j, \quad \frac{\partial w_j}{\partial x}, \quad v_j\right\}^T = [A]\{C\} \tag{2.1.2.7}$$

The terms of matrix [*A*] are determined using Equation 6 where *x* in matrix [R] is replaced by definite values x_i and x_j; the nodal coordinates corresponding respectively, to nodes *i* and *j*, see Figure 2.

By multiplying Equation (8) by $[A]^{-1}$, one obtains the vector $\{C\}$ as a function of the nodal displacements of the considered finite element, as follows:

$$\{C\} = [A]^{-1}\{\delta\}^e \tag{2.1.2.8}$$

Equation (7) is then rewritten as:

$$\begin{Bmatrix} U(x,\theta) \\ W(x,\theta) \\ V(x,\theta) \end{Bmatrix} = [T_n][R][A]^{-1}\{\delta\}^e = [N]\{\delta\}^e \tag{2.1.2.9}$$

where $[N]$ is the shape functions matrix of a cylindrical finite element.

2.1.3.Kinematics Relations

Strain-displacement relations for the cylindrical shell are given by [1]:

$$\{\varepsilon\} = \begin{Bmatrix} \varepsilon_x \\ \varepsilon_\theta \\ 2\bar{\varepsilon}_{x\theta} \\ \kappa_x \\ \kappa_\theta \\ 2\bar{\kappa}_{x\theta} \end{Bmatrix} = \begin{Bmatrix} \frac{\partial U}{\partial x} \\ \frac{1}{R}\frac{\partial V}{\partial \theta} + \frac{W}{R} \\ \frac{\partial V}{\partial x} + \frac{1}{R}\frac{\partial U}{\partial \theta} \\ -\frac{\partial^2 W}{\partial x^2} \\ -\frac{1}{R^2}\frac{\partial^2 W}{\partial \theta^2} + \frac{1}{R^2}\frac{\partial V}{\partial \theta} \\ -\frac{2}{R}\frac{\partial^2 W}{\partial x \partial \theta} + \frac{3}{2R}\frac{\partial V}{\partial \theta} - \frac{1}{2R^2}\frac{\partial V}{\partial \theta} \end{Bmatrix} \tag{2.1.2.10}$$

Substituting the displacements given in Equation (10) into the strain-displacement relationship, we obtain an expression for the strain vector as a function of nodal displacements.

$$\{\varepsilon\} = \begin{bmatrix} [T_n] & 0 \\ 0 & [T_n] \end{bmatrix} [Q][A^{-1}] \begin{Bmatrix} \delta_i \\ \delta_j \end{Bmatrix} = [B] \begin{Bmatrix} \delta_i \\ \delta_j \end{Bmatrix} \tag{2.1.2.11}$$

The terms of matrix $[Q]$ of order 6×8 are given in reference [18] and the matrix $[B]$ is defined in Equation (12).

2.1.4. Constitutive Equations

In the case of an anisotropic material, the resultant stress vector may be expressed as follows:

$$\{\sigma\} = [P]\{\varepsilon\} \tag{2.1.2.12}$$

where $[P]$ is the elasticity matrix (6×6) expressed as:

$$[P] = \begin{bmatrix} P_{11} & P_{12} & 0 & P_{14} & P_{15} & 0 \\ P_{21} & P_{22} & 0 & P_{24} & P_{25} & 0 \\ 0 & 0 & P_{33} & 0 & 0 & P_{36} \\ P_{41} & P_{42} & 0 & P_{44} & P_{45} & 0 \\ P_{51} & P_{52} & 0 & P_{54} & P_{55} & 0 \\ 0 & 0 & P_{63} & 0 & 0 & P_{66} \end{bmatrix} \tag{2.1.2.13}$$

The elements P_{ij} of matrix $[P]$ are elasticity coefficients for an anisotropic material which depend on the mechanical properties of the shell. If the material is isotropic the non-zero elements of matrix $[P_{ij}]$ are:

$$P_{11} = P_{22} = D \qquad P_{12} = P_{21} = \nu D \qquad P_{33} = (1-\nu)D/2$$
$$P_{44=}P_{55} = K \qquad P_{45} = P_{54} = \nu K \qquad P_{66} = (1-\nu)K/2$$

with:

$K = Et^3/(12(1-\nu^2)$ and $D = Et/(1-\nu^2)$, E is Young's modulus, t is shell thickness and ν is Poisson's ratio. It is important to note that this model can take into account the anisotropy of the shells provided that their mechanical properties are known.

2.1.5. Elementary Mass and Stiffness Matrices

The elementary mass $[m_s]^e$ and stiffness $[k_s]^e$ matrices may be calculated using the standard finite element method procedure as follows [4]:

$$[m_s]^e = \rho_s t \iint_A [N]^T[N]dA \tag{2.1.2.14}$$

$$[k_s]^e = \iint_A [B]^T[P][B]dA \tag{2.1.2.15}$$

where: ρ_s is the density of the shell, t is the finite element thickness and A is the finite element area defined by $R_e d\theta dx$ (see Figure 2), $[N]$ is the shape functions matrix, $[B]$ is the matrix defined in Equation (12) and $[P]$ is the elasticity matrix.

Substituting the matrices $[N]$ and $[B]$ by their expressions into Equations (15) and (16) we obtain:

$$[m_s]^e = \rho_s t[[A]^{-1}]^T \left(\pi R_e \int_0^{l_e} [R]^T[R]dx\right)[A]^{-1} \tag{2.1.2.16}$$

$$[k_s]^e = [[A]^{-1}]^T \left(\pi R_e \int_0^{l_e} [Q]^T[P][Q]dx\right)[A]^{-1} \tag{2.1.2.17}$$

where R_e and l_e are the radius and the length of the shell element considered, see Figure 2. The elementary matrices $[m_s]^e$ and $[k_s]^e$ are calculated by analytical integration over x and θ.

2.2. Conical Shell Model

The same approach is used to formulate the conical element. However, the equilibrium equations and displacement functions are specific to conical shells.

2.2.1. Equations of Motion

The conical part of the combined shell is modeled using a conical finite element, see Figure 3. The equations of motion of conical shells are given in terms of the three displacements ($\overline{U}, \overline{V}, \overline{W}$) of the mean surface of the shell and in terms of the elasticity matrix $[P]$ as follows [5]:

$$S_1\left(\overline{U}, \overline{V}, \overline{W}, B_{ij}\right) = 0 \tag{2.2.1.a}$$

$$S_2\left(\overline{U}, \overline{V}, \overline{W}, B_{ij}\right) = 0 \tag{2.2.1.b}$$

$$S_3\left(\overline{U}, \overline{V}, \overline{W}, B_{ij}\right) = 0 \tag{2.2.1.c}$$

where:

S_k (k = 1, 2,3) are three linear differential operators, the form of which is given fully in Appendix B. B_{ij} terms are the components of an anisotropic matrix of elasticity $[P]$, see reference [6].

The equations of motion are developed for conical shells with linearly variable thicknesses as shown in Figure 3. This geometry enables us to use the equilibrium equations to determine the displacement functions [5]. However, it is possible to study the case of truncated conical shells with a constant thickness by introducing the thickness proportionality coefficient δ. This coefficient is determined such that the constant thickness is found in the middle of each circumferential finite element. This approximation does not affect the quality of results [6]. Therefore, the finite element used to model the dynamic behaviour of the conical part of the shell is a truncated cone with variable thickness defined by two line-nodes, i and j. Each node has four degrees of freedom: three displacements ($\overline{u}_i, \overline{v}_i$ and $\overline{w}_i$) and one rotation $\partial\overline{w}_i/\partial x$ oriented as shown in Figure 3. The δ coefficient for each element is expressed by [6]:

$$\delta = \frac{2t}{(x_j - x_i)} \tag{2.2.1.2}$$

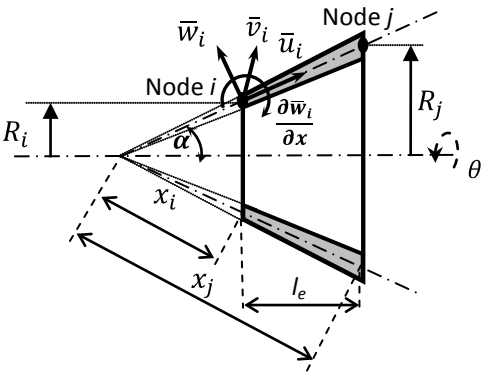

Fig. 3 Geometry and nodal displacements of the conical finite element

2.2.2. Displacement Functions

As assumed for cylindrical element, the displacement functions are obtained by combining Fourier series and the finite element method. According to the circumferential direction, they are expressed by:

$$\begin{Bmatrix} \bar{U}(x,\theta) \\ \bar{W}(x,\theta) \\ \bar{V}(x,\theta) \end{Bmatrix} = \begin{bmatrix} \cos(n\theta) & 0 & 0 \\ 0 & \cos(n\theta) & 0 \\ 0 & 0 & \sin(n\theta) \end{bmatrix} \begin{Bmatrix} \bar{U}(x) \\ \bar{W}(x) \\ \bar{V}(x) \end{Bmatrix} = [T_n] \begin{Bmatrix} \bar{U}(x) \\ \bar{W}(x) \\ \bar{V}(x) \end{Bmatrix} \qquad (2.2.1.3)$$

where $\bar{U}(x), \bar{V}(x)$ and $\bar{V}(x)$ are only functions of x.

Substituting the displacement functions into Equation (19) and working out derivatives with respect to θ, one obtains three ordinary differential equations. The solutions of these equations have the following general form [7]:

$$\begin{Bmatrix} \bar{U}(x) \\ \bar{V}(x) \\ \bar{W}(x) \end{Bmatrix} = \left(\frac{x}{l_e}\right)^{\frac{\bar{\lambda}-1}{2}} \begin{Bmatrix} \bar{A} \\ \bar{B} \\ \bar{C} \end{Bmatrix} \qquad (2.2.1.4)$$

where:

l_e is the length of the considered element (see Figure 3), and $\bar{A}, \bar{B}, \bar{C}$ and $\bar{\lambda}$ are unknown complex numbers.

Substituting $\bar{U}(x), \bar{V}(x)$ and $\bar{V}(x)$ into the equilibrium equations we obtain the algebraic system written as:

$$\begin{bmatrix} D_{11} & D_{12} & D_{13} \\ D_{21} & D_{22} & D_{23} \\ D_{31} & D_{32} & D_{33} \end{bmatrix} \begin{Bmatrix} \bar{A} \\ \bar{B} \\ \bar{C} \end{Bmatrix} = [D] \begin{Bmatrix} \bar{A} \\ \bar{B} \\ \bar{C} \end{Bmatrix} = \begin{Bmatrix} 0 \\ 0 \\ 0 \end{Bmatrix} \qquad (2.2.1.5)$$

The nine terms of matrix $[D]$ are given in Appendix B. For non-trivial solution of the Equations (23) the determinant of matrix [*D*] must be null. This leads to the following characteristic equation:

$$h_8\bar{\lambda}^8 + h_6\bar{\lambda}^6 + h_4\bar{\lambda}^4 + h_2\bar{\lambda}^2 + h_0 = 0 \qquad (2.2.1.6)$$

The coefficients h_j (for j=0, 2, 4, 6 and 8) are given in [6]. Solution of this characteristic equation provides eight roots $\bar{\lambda}_j$ (j=1-8). Each root constitutes a solution of the equilibrium equations. The complete solution is the linear combination of these equations with the constants $\bar{A}_j, \bar{B}_j$ and $\bar{C}_j$ (j = 1, 8) as follows:

$$\begin{Bmatrix} U(x) \\ V(x) \\ W(x) \end{Bmatrix} = \sum_{j=1}^{j=8} \left(\frac{x}{l_e}\right)^{\frac{\bar{\lambda}_j-1}{2}} \begin{Bmatrix} \bar{A}_j \\ \bar{B}_j \\ \bar{C}_j \end{Bmatrix} \qquad (2.2.1.7)$$

Since $\bar{A}_j$, $\bar{B}_j$ and $\bar{C}_j$are not independent, it is possible to express them as a function of $\bar{C}_j$, using complex constants $\bar{\alpha}_j$ and $\bar{\beta}_j$ as follows:

$$\bar{A}_j = \bar{\alpha}_j\bar{C}_j \text{ and } \bar{B}_j = \bar{\beta}_j\bar{C}_j \qquad j=1\text{-}8 \qquad (2.2.1.8)$$

The values of $\bar{\alpha}_j$ and $\bar{\beta}_j$ can be obtained from the system Equation (23) by introducing relations of Equation (28) for each value of $\bar{\lambda}_j$.

The displacements $\bar{U}(x), \bar{V}(x)$ and $\bar{V}(x)$ may be finally written as:

$$\begin{Bmatrix} \bar{U}(x) \\ \bar{V}(x) \\ \bar{W}(x) \end{Bmatrix} = [\bar{R}]\{\bar{C}\} \qquad (2.2.1.9)$$

where:

$[\bar{R}]$ is a matrix of order (3×8) and is given in reference [6]. The vector $\{\bar{C}\}$ contains eight constants of the problem which may be expressed as functions of nodal displacements. For a conical finite element, the nodal displacement vector associated to circumferential mode n and nodes *i* and *j* is given by (see Figure 3):

$$\{\bar{\delta}\}^e = \left\{\bar{u}_i, \quad \bar{w}_i, \quad \frac{\partial \bar{w}_i}{\partial x}, \quad \bar{v}_i, \quad \bar{u}_j, \quad \bar{w}_j, \quad \frac{\partial \bar{w}_j}{\partial x}, \quad \bar{v}_j\right\}^T = [\bar{A}]\{\bar{C}\} \tag{2.2.1.10}$$

The terms of $[\bar{A}]$ can be obtained by replacing *x* by the nodal coordinates x_i and x_j corresponding to nodes *i* and *j*, respectively. Now, pre-multiplying by $[\bar{A}]^{-1}$ one obtains:

$$\{\bar{C}\} = [\bar{A}]^{-1}\{\bar{\delta}\}^e \tag{2.2.1.11}$$

The final displacement functions may be therefore written as:

$$\begin{Bmatrix} \bar{U}(x,\theta) \\ \bar{V}(x,\theta) \\ \bar{W}(x,\theta) \end{Bmatrix} = [T_n][\bar{R}][\bar{A}]^{-1}\{\bar{\delta}\}^e = [\bar{N}]\{\bar{\delta}\}^e \tag{2.2.1.12}$$

where $[\bar{N}]$ is the shape functions matrix of a conical finite element.

2.2.3. Kinematics Relations

Strain-displacement relations for a conical shell are given by [5]:

$$\begin{Bmatrix} \varepsilon_x \\ \varepsilon_\theta \\ 2\bar{\varepsilon}_{x\theta} \\ \kappa_x \\ \kappa_\theta \\ 2\bar{\kappa}_{x\theta} \end{Bmatrix} = \begin{Bmatrix} \dfrac{\partial \bar{U}}{\partial x} \\ \dfrac{1}{x\sin(\alpha)}\dfrac{\partial \bar{V}}{\partial \theta} + \dfrac{\bar{U}}{x} + \dfrac{\bar{W}\cos(\alpha)}{x} \\ \dfrac{\partial \bar{V}}{\partial x} + \dfrac{1}{x\sin(\alpha)}\dfrac{\partial \bar{U}}{\partial \theta} - \dfrac{\bar{V}}{x} \\ -\dfrac{\partial^2 \bar{W}}{\partial x^2} \\ \dfrac{\cos(\alpha)}{(x\sin(\alpha))^2}\dfrac{\partial \bar{V}}{\partial \theta} - \dfrac{1}{(x\sin(\alpha))^2}\dfrac{\partial^2 \bar{W}}{\partial \theta^2} - \dfrac{1}{x}\dfrac{\partial \bar{W}}{\partial x} \\ -\dfrac{2}{x\sin(\alpha)}\dfrac{\partial^2 \bar{W}}{\partial x \partial \theta} + \dfrac{3\cot(\alpha)}{2x}\dfrac{\partial \bar{V}}{\partial x} - \dfrac{\partial \bar{U}}{\partial \theta}\dfrac{\cos(\alpha)}{2(x\sin(\alpha))^2} + \dfrac{2\sin(\alpha)}{(x\sin(\alpha))^2}\dfrac{\partial \bar{W}}{\partial \theta} - \dfrac{3}{2}\dfrac{\cot(\alpha)}{x^2}\bar{V} \end{Bmatrix} \tag{2.2.1.13}$$

Substituting the displacements given in Equation (30) into the strain-displacement relationship (31), we obtain:

$$\{\epsilon\} = \begin{bmatrix} [T_n] & 0 \\ 0 & [T_n] \end{bmatrix}[\bar{Q}][\bar{A}^{-1}]\{\bar{\delta}\}^e = [\bar{B}]\{\bar{\delta}\}^e \tag{2.2.1.14}$$

The terms of matrix $[\bar{Q}]$ of order 6×8 are given in reference [5].

2.2.4. Elementary Mass and Stiffness Matrices

Equation (13) applies also here to express the stress-strain relationship in the case of a conical shell. The elasticity matrix is the same as that given in Equation (14) and the material anisotropy may also be considered in the conical model. By substituting the matrices $[\bar{N}]$ and $[\bar{B}]$ by their expressions into Equations (15) and (16) we obtain:

$$[\bar{m}_s]^e = \rho_s \int_A [[\bar{A}]^{-1}]^T [\bar{R}]^T \begin{bmatrix} [T_n] & [0] \\ [0] & [T_n] \end{bmatrix}^T \begin{bmatrix} [T_n] & [0] \\ [0] & [T_n] \end{bmatrix} [\bar{R}][\bar{A}]^{-1} t dA \tag{2.2.4.1}$$

$$\left[\bar{k}_s\right]^e = \int_A [[\bar{A}]^{-1}]^T [\bar{Q}]^T \begin{bmatrix} [T_n] & [0] \\ [0] & [T_n] \end{bmatrix}^T [P] \begin{bmatrix} [T_n] & [0] \\ [0] & [T_n] \end{bmatrix} [\bar{Q}][\bar{A}]^{-1} dA \tag{2.2.4.2}$$

where:

ρ_s and t are the density and the thickness of the conical shell, respectively, dA is a differential area in the considered element defined by $dA = xsin(\alpha)d\theta dx$ (see Figure 3), $[P]$ is the elasticity matrix, and matrices $[\mathrm{T_n}]$, $[\overline{\mathrm{R}}]$, $[\overline{\mathrm{A}}]^{-1}$, and $[\overline{\mathrm{Q}}]$ are defined in Equations (21), (27), (29) and (32), respectively.

3. Fluid Modeling

The combined conical-cylindrical shell studied here may be fully or partially filled by heavy fluid without net flow rate. The presence of fluid inside the shell affects its dynamic behaviour significantly. The fluid pressure applied on the combined shell is coupled with elastic deformation of the shell and is introduced in the governing equations as an inertial force.

The fluid mathematical models of conical and cylindrical finite elements are based on the following assumptions: (i) the fluid is incompressible, (ii) the fluid flow is potential, (iii) the mathematical model is limited to small deformations, (iv) the fluid pressure is purely normal to the shell wall since fluid is inviscid (there is no shear) and (v) the shell semi-vertex angle may not be equal to zero. The free surface effect is not considered where applicable.

3.1. Fluid Model for Cylindrical Finite Elements

Based on the fluid assumptions cited above, the velocity potential must satisfy the Laplace equation. This relation is expressed in the cylindrical coordinate system by [1]:

$$\frac{1}{r}\frac{\partial}{\partial r}\left(\frac{r\partial\phi(x,\theta,r,t)}{\partial r}\right)+\frac{1}{r^2}\frac{\partial^2\phi(x,\theta,r,t)}{\partial\theta^2}+\frac{\partial^2\phi(x,\theta,r,t)}{\partial x^2}=0 \tag{3.1.1}$$

where:

$\phi(x,\theta,r,t)$ is the potential function, and x, θ and r are the coordinates in the axial, circumferential and radial directions of the cylinder, respectively.

The components of the flow velocity in the case of potential flow theory without a net flow rate may be expressed as follows [10]:

$$V_r=\frac{\partial\emptyset}{\partial r}\qquad V_\theta=\frac{1}{r}\frac{\partial\emptyset}{\partial\theta}\qquad V_x=\frac{\partial\emptyset}{\partial x} \tag{3.1.2}$$

$\mathrm{V_x}, \mathrm{V_\theta}$ and $\mathrm{V_r}$ are respectively the axial, tangential and radial components of the fluid velocity.

The fluid pressure at the solid–fluid interface ($r=R_e$) may be expressed using Bernoulli's equation as follows [10]:

$$P|_{r=R_e}=-\rho_f\left.\frac{\partial\emptyset}{\partial t}\right|_{r=R_e} \tag{3.1.3}$$

where ρ_f is the fluid density.

Two boundary conditions characterize the fluid conditions in this case. The first ensures a finite solution on the axis at r=0 and is expressed by:

$$\left.\frac{\partial\emptyset}{\partial \mathrm{r}}\right|_{\mathrm{r}=0}=0 \tag{3.1.4}$$

The second boundary condition, known as impermeability condition, ensures a permanent contact between the shell surface and the peripheral fluid layer, which should be:

$$V_r|_{r=R_e}=\left.\frac{\partial\emptyset}{\partial r}\right|_{r=R_e}=\left.\frac{\partial W}{\partial t}\right|_{r=R_e} \tag{3.1.5}$$

The following separate variable relation is assumed for the potential velocity function:

$$\emptyset(x,\theta,r,t) = F(r)S(x,\theta,t) \tag{3.1.6}$$

where F(r) and S(x, θ, t) are unknown functions. Equation (7) allows us to express the radial displacement by the following relation:

$$W(x,r,\theta,t) = \sum_{j=1}^{8} C_j e^{\frac{\lambda_j x}{l_e}} \cos(n\theta)\, e^{i\omega t} \tag{3.1.7}$$

where i is a complex number, i2=-1 and ω is the natural frequency.

By substituting Equations (40) into the impermeability condition of Equation (39), we determine the function S(x, θ, t). Replacing again the function S(x, θ, t) into Equation (40), the potential velocity function becomes:

$$\emptyset(x,r,\theta,t) = \sum_{j=1}^{j=8} \frac{F_j(r)}{\left[\partial F_j(R_e)/\partial r\right]} \frac{\partial W_j}{\partial t} \tag{3.1.8}$$

The fluid pressure may therefore be rewritten using Equation (37) as:

$$P|_{r=R} = -\rho_f \sum_{j=1}^{j=8} \frac{F_j(r)}{\left[\partial F_j(R_e)/\partial r\right]} \frac{\partial^2 W_j}{\partial t^2} \tag{3.1.9}$$

Equations (42) and (43) show that the fluid pressure is coupled at the interface to the radial displacement of the shell. However it is necessary to define the function *F(r)*. By introducing the velocity potential function $\emptyset(x,\theta,r,t)$ into Equation (35), one obtains:

$$\sum_{j=1}^{j=8} \left[\frac{\partial^2 F_j(r)}{\partial r^2} + \frac{\partial F_j(r)}{\partial r} - \frac{n^2}{r^2} F_j(r) \left(1 + \left(i\frac{\lambda_j}{l_e}\right)^2\right)\right] = 0 \tag{3.1.10}$$

The general solution of Equation (44) is given by:

$$F_j(r) = AJ_n(im_j r) + BY_n(im_j r) \tag{3.1.11}$$

with:

$J_n(im_j r)$ and $Y_n(im_j r)$ are, respectively, the Bessel function of the first and second kind of order n. *A* and *B* are unknown constants and the parameter $m_j = \frac{\lambda_j}{l_e}$.

In the case of internal fluid, the solution of Equation (44) must be finite on the axis of the shell (r=0). This means that we have to set the constant *B* equal to zero [9]. The solution of the differential Equation (44) becomes:

$$F_j(r) = AJ_n(im_j r) \tag{3.1.12}$$

Finally, we obtain the fluid pressure equation at the solid-fluid interface as follows:

$$P|_{r=R} = -\rho_f \sum_{j=1}^{j=8} \frac{J_n(im_j r)}{\left[\frac{\partial}{\partial r}(J_n(im_j R))\right]} \frac{\partial^2 W_j}{\partial t^2} = -\rho_f \sum_{j=1}^{j=8} Z_j \frac{\partial^2 W_j}{\partial t^2} \tag{3.1.13}$$

Based on standard finite element procedure, the fluid-induced force vector may be expressed for one finite element using the following relation:

$$\{F\}^e = \int_A [N]\{P\} dA \tag{3.1.14}$$

where: $\{F\}^e$ is the elementary load vector of order (8×1), [*N*] is the shape functions matrix of the finite element defined in Equation (10), and $\{P\}$ is a vector expressing the pressure applied by the fluid on the cylindrical shell in Equation (51). The radial pressure in vector $\{P\}$ is the only non-zero component.

By substituting matrices [*N*] and $\{P\}$ in Equation (48), we obtain:

$$\{F\}^e = -\rho_f \int_A \left[Z_f\right]^T [[A]^{-1}]^T [R]^T [T_n]^T [T_n] \left[R_f\right] \left[A_f\right]^{-1} \{\ddot{\delta}\}^e dA \tag{3.1.15}$$

where:

$[R_f]$ is a matrix of order (3×8) that contains only the second line of matrix $[R]$ associated with the radial displacement, $[A_f]^{-1}$ is a matrix of order (8×8) obtained using Equations (8) to (10) by considering only the radial displacement *W*, vector $\{Z_f\}$ of order (1×8) contains the eight components of Z_j written in vector form (see Equation 47).

After integration, the last equation may be rewriten as:

$$\{F\}^e = [[A]^{-1}]^T[S_f][A_f]^{-1}\{\ddot{\delta}\}^e \tag{3.1.16}$$

The $[S_f]$ matrix is given in reference [10]. The added mass matrix of the cylindrical element due to the fluid is therefore:

$$[m_f] = [[A]^{-1}]^T[S_f][A_f]^{-1} \tag{3.1.17}$$

3.2. Fluid Model for a Conical Finite Element

Given the fluid assumptions mentioned above, the velocity potential may be expressed in the system of conical coordinates system by [11]:

$$\nabla^2\emptyset = \frac{2}{x}\frac{\partial\emptyset}{\partial x} + \frac{\partial^2\emptyset}{\partial x^2}\frac{1}{x^2(\sin\beta)^2}\frac{\partial^2\emptyset}{\partial\theta^2} + \frac{1}{x^2\tan\beta}\frac{\partial\emptyset}{\partial\beta} + \frac{1}{x^2}\frac{\partial^2\emptyset}{\partial\beta^2} \tag{3.2.1}$$

where: $\emptyset(x,\theta,\beta)$ is the potential function, and x, θ and β are the conical coordinates, see Figure 4.

In the case of fluid at rest, the Bernoulli's equation for conical coordinates applied at the middle surface of a conical shell is given by [6]:

$$P|_{\beta=a} = -\rho_f \left.\frac{\partial\emptyset}{\partial t}\right|_{\beta=a} \tag{3.2.2}$$

where :

β is the coordinate along the cone semi-vertex angle α and $a = \alpha - \tan(x/2h)$ is the half-angle at the interface between the fluid and the middle surface of the conical shell, see Figures 3 and 4.

The flow velocity components in the case of potential flow without a net flow rate are expressed in conical coordinates by [8]:

$$V_x = \frac{\partial\emptyset}{\partial x} \qquad V_\theta = \frac{1}{xsin\alpha}\frac{\partial\emptyset}{\partial\theta} \qquad V_\beta = \frac{1}{x}\frac{\partial\emptyset}{\partial\beta} \tag{3.2.3}$$

In order to impose the fluid-structure coupling, the impermeability condition for conical coordinates should be applied at the interface as follows [12]:

$$V_\beta\big|_{\beta=a} = \frac{1}{x}\left.\frac{\partial\emptyset}{\partial\beta}\right|_{\beta=a} = \left.\frac{\partial\bar{W}}{\partial t}\right|_{\beta=a} \tag{3.2.4}$$

Using Equations (21) and (29), the radial displacement may be rewritten as:

$$\bar{W}(x,\theta,t) = \sum_{j=1}^{j=8}\bar{C}_j y^{\lambda_j - 1}cos\,(n\theta)e^{i\omega t} \tag{3.2.5}$$

Assuming then:

$$\emptyset(x,\theta,\beta,t) = \sum_{j=1}^{j=8} G_j(\beta)T_j(x,\theta,t) \tag{3.2.6}$$

where: $G_j(\beta)$ and $T_j(x,\theta,t)$ are unknown functions.

Substituting the equation (57) into the impermeably condition of Equation (55) we determine the function $T_j(x,\theta,t)$. Introducing this function into Equation (57), one obtains:

$$\bar{\emptyset}(x,\theta,\beta,t) = x\sum_{j=1}^{j=8}\frac{G_j(\beta)}{[\partial G_j(a)/\partial\beta]}\frac{\partial\bar{W}}{\partial t} \tag{3.2.7}$$

Replacing Equation (58) into Equation (52) and solving for a constant x, leads to the following second order ordinary differential equation:

$$\frac{\partial^2 G_j(\beta)}{\partial \beta^2} + \frac{1}{\tan(\beta)}\frac{\partial G_j(\beta)}{\partial \beta} - \frac{n^2}{sin^2(\beta)} G_j(\beta) = 0 \tag{3.2.8}$$

Since the fluid is inside the conical shell, the previous equation may be solved using the Frobenius method. The truncated solution is expressed by Korn and Korn [11] as:

$$G_j(\beta) = A\beta^n \left[1 + \frac{n}{12}\beta^2 + \frac{(5n+7)n}{1440}\beta^4 + \frac{n(n+4)(5n+1)}{51840}\beta^6\right] \tag{3.2.9}$$

Introducing Equation (60) into Equation (58), the potential function becomes:

$$\overline{\emptyset}(x,\theta,\beta,t) = kx\sum_{j=1}^{j=8}\frac{\partial \overline{W}}{\partial t} \tag{3.2.10}$$

with :

$$K = \frac{a}{n}\left(\frac{1+\frac{n}{12}a^2+\frac{(5n+7)n}{1440}a^4+\frac{n(n+4)(5n+1)}{51840}a^6}{1+\frac{(n+2)a^2}{12}+\frac{(n+4)(5n+7)}{1440}a^4+\frac{(n+4)(n+6)(5n+1)}{51840}a^6}\right) \tag{3.2.11}$$

The expression of fluid pressure at the solid-fluid interface may be obtained by replacing the last potential function in Bernoulli's equation (53) as follows:

$$P|_{\beta=a} = -\rho_f k\sum_{j=1}^{j=8} x\frac{\partial^2 \overline{W}_j}{\partial t^2} \tag{3.2.12}$$

This last equation shows that the fluid pressure is coupled at the interface to the radial displacement of the conical shell.

The elementary load vector corresponding to a conical finite element may be calculated by substituting the shape function matrix $[\overline{N}]$ and the fluid pressure *P* of Equation (63) into the standard finite element equation (48). After performing matrix operations, one obtains the following relation:

$$\{F\}^e = -\rho_f \int_A [[\overline{\mathrm{A}}]^{-1}]^{\mathrm{T}}[\overline{R}]^T[T_n]^T[T_n]\left[\overline{R}_f\right][\overline{\mathrm{A}}_{\mathrm{f}}]^{-1}\{\ddot{\delta}\}^{\mathrm{e}}\,\mathrm{dA} \tag{3.2.13}$$

where:

$\left[\overline{R}_f\right]$ is a matrix of order (3×8) that contains only the second line of matrix $[\overline{R}]$ associated with the radial displacement of a conical finite element, $\left[\bar{A}_f\right]^{-1}$ is a matrix of order (8×8) obtained using Equations (29) by considering only the radial displacement $\overline{W}$.

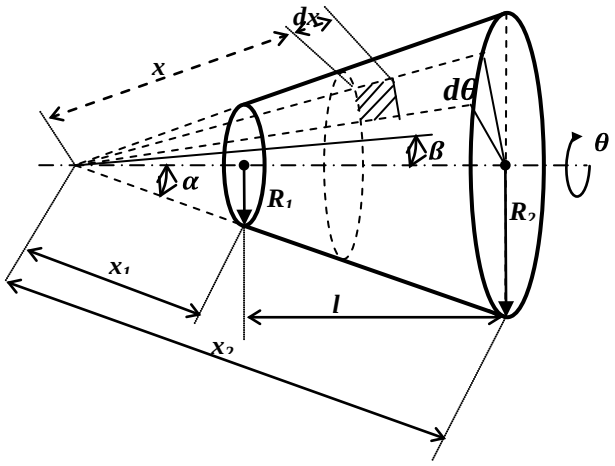

Fig. 4 Fluid and solid coordinates of the truncated-conical shell

The elementary load vector may be rewritten after analytical integration as:

$$\{F\}^e = [[\bar{A}]^{-1}]^T [\bar{S}_f][\bar{A}_f]^{-1}\{\ddot{\delta}\}^e \tag{3.2.14}$$

where $[\bar{S}_f]$ is a matrix of order (8×8) given in reference [6]. The fluid added mass matrix may be deduced from Equation (65) as:

$$[\bar{m}_f] = [[\bar{A}]^{-1}]^T [\bar{S}_f][\bar{A}_f]^{-1} \tag{3.2.15}$$

3.3. Transformation to a Global System

As shown in Figure 5, the nodal displacements of the conical finite element and those of the cylindrical element are not defined in coincident coordinate systems. However, the finite element method requires that, before assembling the global matrices that will describe the dynamic equations of motion, the displacements as well as the nodal loads and elementary matrices must be defined in a single global coordinate system [4]. This geometrical transformation does not apply to conical finite elements having the same semi-vertex α, see Figure 4. Therefore, the nodal displacements of cylindrical elements may be written in terms of nodal displacements of conical elements as follows:

$$\begin{Bmatrix} u_i \\ w_i \\ \frac{\partial w_i}{\partial x} \\ v_i \end{Bmatrix} = \begin{bmatrix} cos\,(\alpha) & -sin\,(\alpha) & 0 & 0 \\ sin\,(\alpha) & cos\,(\alpha) & 0 & 0 \\ 0 & 0 & 1 & 0 \\ 0 & 0 & 0 & 1 \end{bmatrix} \begin{Bmatrix} \bar{u}_i \\ \bar{w}_i \\ \frac{\partial \bar{w}_i}{\partial x} \\ \bar{v}_i \end{Bmatrix} = [T] \begin{Bmatrix} \bar{u}_i \\ \bar{w}_i \\ \frac{\partial \bar{w}_i}{\partial x} \\ \bar{v}_i \end{Bmatrix} \tag{3.3.1}$$

where:

$[T]$ is geometrical transformation matrix of order (4×4).

The elementary matrices of cylindrical finite elements must also be transformed to the global coordinate system as follows [4]:

$$[\bar{k}]^e = \begin{bmatrix} [T] & [0] \\ [0] & [T] \end{bmatrix}^T [k]^e \begin{bmatrix} [T] & [0] \\ [0] & [T] \end{bmatrix} \tag{3.3.2}$$

$$[\bar{m}]^e = \begin{bmatrix} [T] & [0] \\ [0] & [T] \end{bmatrix}^T [m]^e \begin{bmatrix} [T] & [0] \\ [0] & [T] \end{bmatrix} \tag{3.3.3}$$

where :

$[k]^e$ and $[m]^e$ are respectively, the stiffness and mass matrices of the cylindrical element calculated using Equations (15 and 16), and $[\bar{k}]^e$ and $[\bar{m}]^e$are the corresponding matrices in global coordinates.

In addition, due to the fact that the fluid pressure is coupled to the second time derivative of the radial displacement of the shell (see Equation (47)), the fluid added mass matrix of cylindrical element can be transformed to the global coordinate system as follows:

$$[\bar{\bar{m}}_f]^e = [m_f]^e \begin{bmatrix} [T_f] & [0] \\ [0] & [T_f] \end{bmatrix} \tag{3.3.4}$$

where: $[T_f]$ is the transformation matrix of fluid added mass. It takes into account only the radial displacement as follows:

$$[T_f] = \begin{bmatrix} 0 & -\sin\,(\alpha) & 0 & 0 \\ 0 & cos\,(\alpha) & 0 & 0 \\ 0 & 0 & 0 & 0 \\ 0 & 0 & 0 & 0 \end{bmatrix} \begin{Bmatrix} \bar{u}_i \\ \bar{w}_i \\ \frac{\partial \bar{w}_i}{\partial x} \\ \bar{v}_i \end{Bmatrix} \tag{3.3.5}$$

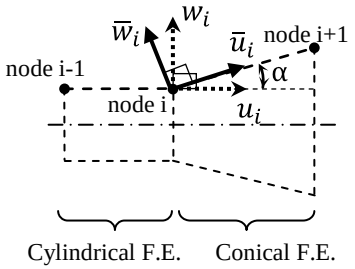

Fig. 5 Elementary conical and cylindrical coordinate transformation

4. Global Matrices and Eigenvalue Problem

The fluid-structure coupled system is governed by the following system of equations [9]:

$$\left[[M_s] - \left[M_f\right]\right]\{\ddot{\delta}_g\} + [K_s]\{\delta_g\} = \{0\} \tag{3.3.6}$$

where :

$[M_s], [K_s]$ are respectively, the global mass and stiffness matrices for the solid shell, $[\mathrm{M_f}]$ is the global matrix of the fluid added mass and $\{\delta_g\}$ is the global displacement vector. The global matrices $[M_s]$, $\left[M_f\right]$ and $[K_s]$ for the whole of the structure are obtained by superimposing the elementary matrices using standard finite element assembling techniques. For the present model, they are complex square matrices of order (4N-F).

where: N is the number of nodes in the structure and F is the number of constraints applied.

The natural frequencies and the mode shapes of the coupled fluid-structure system may be obtained by solving the following eigenvalue problem:

$$\left(\left[[\mathrm{M_s}] - [\mathrm{M_f}]\right] + \Lambda[\mathrm{K_s}]\right)\{\delta_\mathrm{g}\} = \{0\} \tag{3.3.7}$$

where: $\Lambda = -\frac{1}{\omega^2}$ and ω is the natural frequency.

5. Numerical Results and Discussion

To calculate the natural frequencies and mode shapes of the combined conical-cylindrical shell in a vacuum and when coupled with fluid, a computer program in FORTRAN language has been developed based on the theoretical model presented above.

The numerical results were first calculated for the structure without fluid to ascertain that the dynamic behaviour of the structure in a vacuum is predicted correctly. The fluid-structure interaction model is subsequently used to calculate the natural frequencies of a combined shell totally filled with fluid. The obtained results are validated and the solution mesh-independency study is performed using the present model for each case.

5.1. Empty Shell

The first set of calculations is a combined conical-cylindrical shell clamped at both ends, see Figure 6. The mechanical properties of the shell are: Young's modulus E=69 GPa, material density ρ_s=2700 kg/m^3, Poisson's ratio $\nu = 0.3$ and shell thickness = 3 mm. The geometry and the dimensions are illustrated in Figure 6.

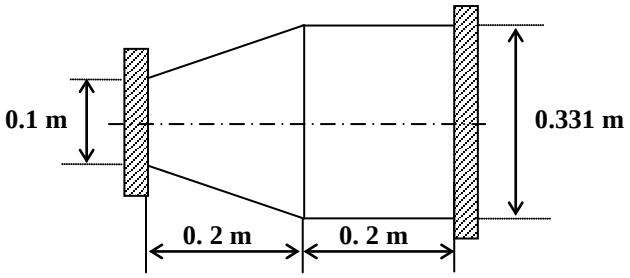

Fig. 6 Geometric shape and dimensions of the combined conical-cylindrical shell in vacuo.

The natural frequencies obtained by the present model are compared in Table 1 to those of ANSYS software calculated using the quadrilateral finite element 'SHELL181'. The results are in very good agreement. A mesh size convergence study has been conducted to determine the requisite number of finite elements for precise determination of the natural frequencies. The results show that only forty finite elements are sufficient to reach the mesh independent solution. A semi-analytical formulation of axisymmetric shells is therefore extremely advantageous compared to the usual finite element approach.

Table 1: Fundamental frequencies f(Hz) of a combined conical-cylindrical shell clamped at both ends (Figure 6)

Circumf. mode (n)	Present method				ANSYS software
	Mesh size (conical+cylindrical F. E.)				
	(6+4)*	(20+10)*	(25+15)*	(40+20)*	5376 F.E. 'SHELL181'
	f(Hz)	f(Hz)	f(Hz)	f(Hz)	f(Hz)
2	1965.43	1488.27	1482.59	1477	1430.1
3	1289.34	1066.74	1062.44	1057.87	1034.6
4	959.91	835.32	832.10	828.53	829.6
5	867.58	790.14	788.07	785.76	791.08
6	924.24	866.73	865.53	864.28	876.35
7	891.08	876.00	875.19	874.95	889.81

* The number of F.E. used in the conical part plus the number of F.E used in the cylindrical part of the combined shell.

5.2. Solid-Fluid Model

The second part of the numerical calculations is devoted to validation of the fluid-structure model presented above. To our best knowledge, the only reference that studied the specific dynamic behaviour of a combined conical-cylindrical shell coupled with internal fluid is that of El-Damatty [3]. A small scale model of a combined conical shell was constructed to study the dynamic behaviour of a containment vessel for elevated water tanks, see Figure 7. The natural

frequencies of this structure in a vacuum were calculated first in reference [2] and those of the liquid-filled shell in reference [3]. Both are compared to our results in Tables 2 and 3.

In addition, a second numerical model of fluid-structure interaction was analyzed using ANSYS software release 14. This allowed us to compare our model to various methods and to have more validation data. The solid shell is modeled using the axisymmetric finite element 'SHELL61', see Figure 8 (a) and (b). It is a one-dimensional finite element defined by two nodes. Each node has four degrees of freedom; three translations and one rotation around the tangential direction. The fluid inside the shell is modeled using the axisymmetric finite element 'FLUID81'. It is a bi-dimensional finite element defined by four nodes having three degrees of freedom at each node: translations in the nodal x, y, and z directions. This element is generally used to model fluid contained within vessels having no net flow rate. The density of the contained water is 1000 kg/m^3 and the bulk modulus of the water, at 2.2 GPa is considered here as the elasticity modulus of the fluid finite element.

To reproduce the same boundary conditions as those of structure illustrated in Figure 7, the fluid movement at the bottom of the shell is restricted to the normal direction. The radial displacement of the fluid element nodes at the centerline (r=0) is constrained because of the axisymmetric property of the studied case (see Figure 9.a). The free surface nodes are free to move arbitrarily with the exception of those located at the shell centerline. At the solid-fluid interface, the solid-fluid coincident nodes are coupled by imposing a similar displacement according to the normal direction. This is made by generating one coupled set for each specified degree of freedom label at every pair of coincident nodes.

The mechanical and geometrical properties of the small scale model are: Young's modulus E=69 GPa, material density ρ_s=2700 kg/m^3, Poisson's ratio $\nu = 0.3$, and the diameters of the combined shell at the bottom and top circumferential lines are D_b=0.302 m and D_t=0.5505 m, respectively (see Figure 7). The total height of the model is 0.627 m and its thickness is 3 mm. The boundary conditions are applied on the circumferential line located at the bottom cross section of the shell [3]. The node that coincides with this location has the displacements U_i, V_i and W_i restrained and the rotation $\partial w_i/\partial x$ free.

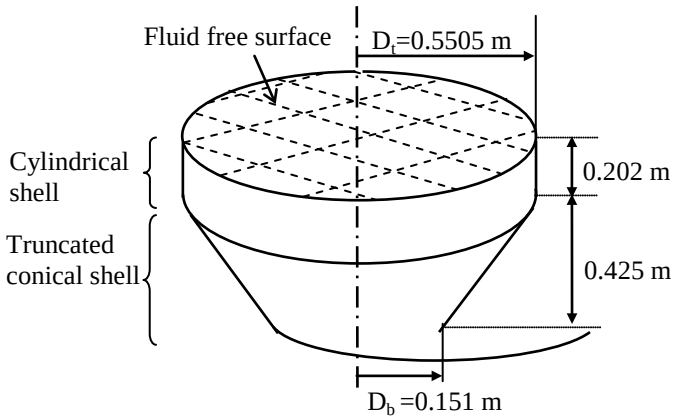

Fig. 7 Geometric shape and dimensions of the combined conical-cylindrical shell fully filled with water.

As can be seen in Table 2, the natural frequencies calculated in a vacuum using the present model are in very good agreement with those calculated numerically in reference [2] and with ANSYS software results. The experimental frequency shows a small difference relative to the numerical one. This discrepancy is justified by the sensitivity of the thin wall structure to geometric imperfections during experimental tests [2].

The natural frequencies of the fully filled shell, calculated using the present model are listed in Table 3 along with the results of reference [3] and those of the ANSYS model. It can be noted that

our first two lower natural frequencies are in very good agreement with those calculated experimentally and numerically in reference [3]. The agreement is within a range of 3.5%. The fundamental frequency

Table 2: Fundamental frequencies f(Hz) of a combined conical-cylindrical shell in a vacuum, see Figure 7.

Circumf. mode (n)	Present method				Ref. [2]		ANSYS software
	Mesh size (conical+cylindrical F. E.)*				F.E.M.	Exp.	
	(12+8)*	(30+10)*	(40+20)*	(40+30)*	256	-	3240 F.E. 'SHELL281'
	f(Hz)	f(Hz)	f(Hz)	f(Hz)	f(Hz)	f(Hz)	f(Hz)
2	79.00	67.21	66.05	66.05	-	-	66.55
3	48.52	43.47	43.63	43.63	46.48	41.6	45.52
4	62.62	61.71	61.62	61.62	-	-	62.80
5	87.61	87.30	87.33	87.30	-	-	87.88

* The number of F.E. used in the conical part plus the number of F.E used in the cylindrical part of the combined shell.

The fundamental frequency corresponds to the circumferential mode n=3 and the second mode to the circumferential mode n=2. This fits perfectly with what was found in reference [3].

The results of the ANSYS model presented in Table 3 have been calculated for the fully filled shell using two different mesh sizes to ensure that the results do not change with the mesh. The first two lower frequencies are in reasonable agreement (less than 12%) with those obtained by the present model. The fundamental mode is presented in Figure 9.b. However, the results discrepancy increases significantly for the higher modes corresponding to circumferential modes n=4 and n=5.

The results obtained using our fluid-structure model show that only forty finite elements are sufficient to reach a mesh-independent solution. The mesh of the conical part of the shell is more refined than that of the cylindrical part since the conical part of the shell is geometrically higher.

The experimental and numerical results cited in Table 3 may be altered by some modeling imperfections. The boundary conditions imposed in the numerical model of reference [3] may be slightly different to those of the experimental model since, in the latter case, the tank wall is fillet-welded at its bottom to a thin circular aluminum plate. This boundary condition is not the perfect equivalent of a simply supported edge as is considered in the numerical model.

Concerning the ANSYS model, it is recommended in reference [13] to keep the finite element 'FLUID81' rectangular during the meshing operation otherwise the accuracy of the results may be altered. Furthermore, it is expected that the fluid-structure ANSYS model provides some low frequencies that represent the internal fluid motions. These frequencies are not considered here as natural frequencies of the fluid-structure coupled system.

Table 3: Fundamental frequencies f(Hz) of a combined conical-cylindrical shell fully filled with water, see Figure 7.

Circumf. mode (n)	Present method				Ref. [3]		ANSYS software model (shell61+Fluid81)	
	Mesh size (conical+cylindrical F. E.)*				F.E.M.	Exp.		
	(12+8)*	(30+10)*	(40+20)*	(40+30)*	-	-	Fluid:20×30 Shell: 30	Fluid:50×60 Shell: 60
2	21.70	18.39	18.03	18.03	18.68	18.4	18.18	18.07
3	**18.10**	**16.31**	**16.06**	**16.04**	**15.46**	**15.6**	**14.00**	**14.15**
4	31.02	30.19	29.75	29.67	-	-	21.15	21.67
5	56.26	54.93	53.54	53.26	49.81	51.9	31.46	32.41

* The number of F.E. used in the conical part plus the number of F.E used in the cylindrical part of the combined shell.

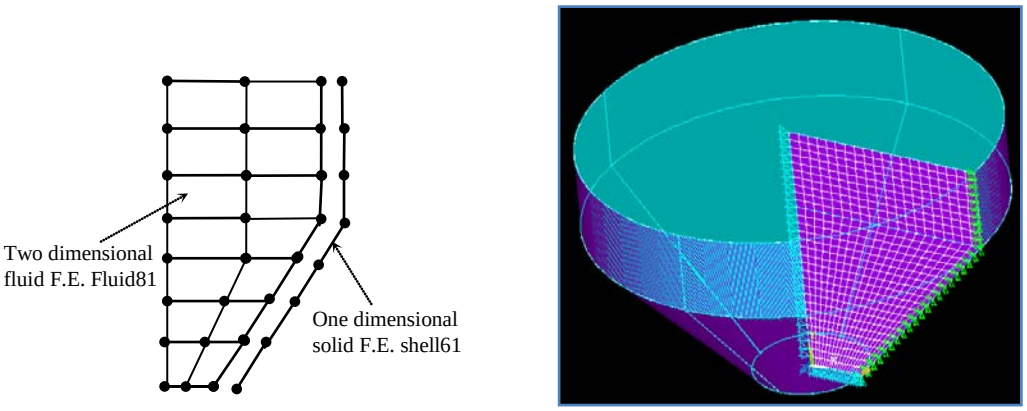

(a) (b)

Fig. 8 Axisymmetric fluid-structure model carried out using ANSYS software.

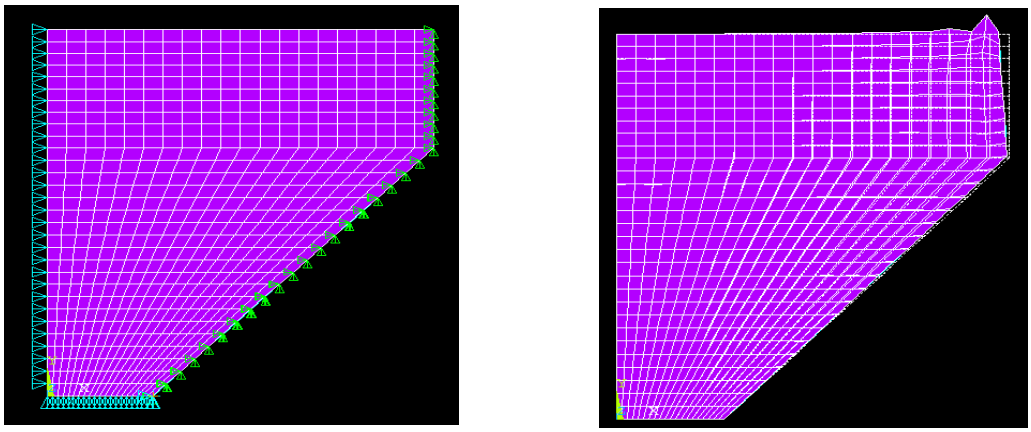

(a) (b)

Fig. 9 Fundamental mode obtained for the combined structure using ANSYS for circumferential mode n=3 (14.15 Hz).

6. Conclusions

The present numerical model predicts the dynamic behaviour of a combined conical-cylindrical shell in a vacuum and when coupled with internal fluid. Although this class of structure is often present in various industrial applications, the appropriate models had not been developed to a useful level. The difficulty of coupling two different fluid-structure interaction models, or to develop a single model valid for both geometries has complicated the task.

The conical and cylindrical models presented here are based on a combination of finite element and classical shell theory. As expected, they provide more accurate results than other proposed methods because their displacement functions are derived from exact solutions of Sanders' shell equilibrium equations. In addition, all solid and fluid matrices are calculated by exact numerical integration. The fluid pressure coupled with solid wall motion was derived by the velocity potential, Bernoulli's equation and the impermeability condition. The elementary matrices

calculated using local coordinates are geometrically transformed to a single global coordinate system.

The numerical results obtained using the developed code show good agreement with other experimental and numerical works available in the literature. The model was tested for different boundary conditions, in a vacuum and when coupled with fluid. The calculated structure may be completely or partially filled with fluid. The requisite number of finite elements needed to reach the mesh independent solution is significantly lower than any other method that uses the usual finite element method.

Finally, it is important to note that we intend to extend this model to the analysis of combined shells subjected to internal and/or external subsonic [39], turbulent [40] and supersonic flows [25].

References

1. *Selmane. A., and Lakis A.A.,* 'Vibration analysis of anisotropic open cylindrical shells subjected to a flowing fluid', *J. Fluid. Struct.,* ***11*** *(1997), 111–134.*
2. *El Damatty A.A., Saafan M.S. and Sweedan A.M.I.,* 'Dynamic characteristics of combined conical-cylindrical shells, Thin-Walled Structures', ***43*** *(2005), 1380–1397.*
3. *El Damatty A.A, Saafan M.S. and Sweedan A.M.I.,* 'Experimental study conducted on a liquid-filled combined conical tank model', *Thin-Walled Structures,* ***43****(2005), 1398–1417.*
4. *Cook R. D., Malkus D. S., Plesha M. E., and Witt R. J., 'Concepts and Applications of Finite Element Analysis'*, 4th edition. John, Wiley & sons, Inc., *2002.*
5. *Lakis A.A., and Ouriche H.,* 'Dynamic analysis of anisotropic conical shells', *Technical Report: EPM/RT-86-36, École Polytechnique of Montreal, 1986.*
6. *Kerboua Y., Lakis A. A., and Hmila M.,* 'Dynamic Analysis of Truncated Conical Shells Subjected to Internal Flowing Fluid', *Applied Mathematical Modelling,* ***34*** *(2010), 791-809.*
7. *Flugge W.,' Stresses in Shells'*, second ed., Springeer-Verlag, Berlin, *1973.*
8. *Lakis A.A., Van Dyke P., and Ouriche H.,* 'Dynamic analysis of anisotropic fluid-filled conical shells', *J. Fluid. Struct.,* ***6*** *(1992), 135–162.*
9. *Lakis A.A., and Neagu S.,* 'Free Surface Effects on the Dynamics of Cylindrical Shells Partially Filled with Liquid', *Journal of Sound and Vibration,* ***207*** *(1997), 175-205.*
10. *Lakis A.A., and Païdoussis M.P.,* 'Free vibration of cylindrical shells partially filled with liquid', *J. Sound,* ***19*** *(1971), 1–15.*
11. *Korn G.A., and Korn T.M., 'Mathematical Handbook for Scientists and Engineers'*, second edition, McGraw-Hill, New York, *1968.*
12. *Lakis A.A., and Van Dyke P. H.,* 'Dynamic analysis of conical shells containing flowing fluid, EPM/RT', *(1988), 88/12.*
13. *Kohnke P., 'Theory reference for mechanical APDL and mechanical applications'*, release 12, *2009.*
14. *Sanders J.L.,* 'An improved first-approximation theory for thin shells', *NASA TR-24, 1959.*
15. *Reissner E.,* 'A new derivation of the equation for the deformation of elastic shells', *Am. J. Math.,****63*** *(1941), 177–184.*
16. *Vlasov V.S.,* 'Basic differential equations in general theory of elastic shells', *NACA-TM, PP-1241-59, 1951.*
17. *Timoshenko S., 'Theory of Plates and Shells'*, McGraw-Hill, New York, *1959.*
18. *Lakis A.A. and Païdoussis N.P.,* 'Dynamic analysis of axially non-uniform thin cylindrical shells', *Journal of Mechanical Engineering Science,* ***14*** *(1972) 49-71.*
19. *Lamb H., 'Hydrodynamics'*, D.P.S. edition. New York, *1945.*
20. *Rayleigh L.,' Theory of sound'*, Second Edition, New York Dover, *1877.*
21. *Berry J.G., and Reissner E.,* 'The effect of an internal compressible fluid column on the breathing vibrations of a thin pressurized cylindrical shell', *Journal of Aerospace Science,* ***25****(1958), 288-294.*
22. *Lindholm U.S., Kana D.D., and Abramson H.N., 'Breathing vibrations of circular cylindrical shell with internal liquid', Journal of the Aerospace Sciences,* ***29*** *(1962), 1052-1059.*
23. *Coale C.W., and Nagano M.,* 'Axisymmetric modes of an elastic cylindrical hemispherical tank partially filled with liquid', *AIAA, Symposium on Structural Dynamics and Aeroelasticity, 1965.*
24. *Lakis A.A., and Païdoussis M.P.,* 'Prediction of the response of a cylindrical shell to arbitrary or boundary-layer-induced random pressure fields', *Journal of Sound and Vibration,* ***25*** *(1972), 1–27.*

25. *Sabri F., and Lakis A. A.,* 'Finite Element Method Applied to Supersonic Flutter of Circular Cylindrical Shells', *AIAA Journal , **48** (2010).*
26. *Mistry J., and Menezes J.C.,* 'Vibration of cylinders partially-filled with liquids', *Journal of Vibration and Acoustics, Transactions of the ASME, **117** (1995), 87-93.*
27. *Amabili M., and Dalpiaz G.,*'Breathing vibrations of a horizontal circular cylindrical tank shell partially filled with liquid', *Journal of Vibration and Acoustics, Transactions of the ASME, **117** (1995), 187-191.*
28. *Jain R.K.,* 'Vibration of fluid-filled orthotropic cylindrical shells', *Journal of Sound and Vibration, **37** (1974), 379-388.*
29. *Ross C.T.F., and Seers A.,* 'Non-linear vibration of ring-stiffened conical shells under external water pressure', *Proceedings of Developments in Computer Aided Design and Modelling for Structural Engineering, Edinburg, (1995), 169–175, UK.*
30. *Nishimura T., and Shingu K.,* 'Theoretical and experimental studies on natural vibration of a submerged conical shell', *Ocean Space Utilization 85, Proceedings of the International Symposium, Tokyo Japan, Springer-Verlag, (1985), 393–400.*
31. *Sweedan A. M. I, and El Damatty A. A.,* 'Experimental identification of the vibration modes of liquid-filled conical tanks and validation of a numerical model, Earthquake Engineering and Structural Dynamics', ***32** (2003), 1407-1430.*
32. *El-Damatty A.A., Korol R.M., and Mirza F.A.,* 'Stability of elevated liquid-filled conical tanks under seismic loading, Part I-Theory, Earthquake Engineering and Structural Dynamics', ***26** (1997), 1191–1208.*
33. *El Damatty A.A., Korol RM, and Mirza FA.,* 'Stability of elevated liquid-filled conical tanks under seismic loading, Part II-Applications', *Earthquake Engineering and Structural Dynamics, **26** (1997), 1209–1229.*
34. *Senthil Kumar D., and Ganesan N.,*'Dynamic analysis of conical shells conveying fluid', *J. Sound Vib., **310** (2008), 38–57.*
35. *Sabri F and Lakis. A. A.,*'Hybrid Finite Element Method Applied to Supersonic Flutter of an Empty or Partially Liquid-Filled Truncated Conical Shell', *Journal of Sound and Vibration, **329** (2010), 302-316.*
36. *Liu M., Liu J., and Cheng Y.,* 'Free Vibration of a Fluid Loaded Ring-Stiffened Conical Shell with Variable Thickness', *Journal of Vibration and Acoustics, **136** (2014).*
37. *Caresta M., and Kessissoglou N. J.,* 'Vibration of Fluid Loaded Conical Shells', *J. Acoust. Soc. Am., **124** (2008), 2068–2077.*
38. *Pan J., Matthews D., Xiao H., Munyard, A., Wang Y., Jin M., and Liu W.,* 'Analysis of underwater vibration of a torpedo-shaped structure subjected to an axial excitation', *Australian Acoustical Society, Proceedings of Acoustics (2011), 527-533.*
39. *Toorani M. H., and Lakis A.A.,*'Dynamic analysis of anisotropic cylindrical shells containing flowing fluid', *Journal of Pressure Vessel Technology, Transactions of the ASME, **123** (2001).*
40. *Esmaïlzadeh M., and Lakis A.A.,* 'Response of an Open Curved thin Shell to Ramdon Pressure Field Arising from a Turbulent Boundary Layer', *Journal of Sound and Vibration, **331**(2012),345-367.*

Appendix A

Equations of motion for a thin anisotropic cylindrical shell

$$L_1(U,V,W,p_{ij}) = p_{11}\frac{\partial^2 U}{\partial x^2} + \frac{p_{12}}{R}\left(\frac{\partial^2 V}{\partial x\partial\theta} + \frac{\partial W}{\partial x}\right) - p_{14}\frac{\partial^3 W}{\partial x^3} + \frac{p_{15}}{R}\left(\frac{\partial^3 W}{\partial x\partial\theta^2} + \frac{\partial^2 V}{\partial x\partial\theta}\right) + \left(\frac{p_{33}}{R} - \frac{p_{63}}{2R^2}\right)\left(\frac{\partial^2 V}{\partial x\partial\theta} + \frac{1}{R}\frac{\partial^2 U}{\partial\theta^2}\right) + \left(\frac{p_{36}}{R^2} - \frac{p_{66}}{2R^3}\right)\left(-\frac{2\partial^3 W}{\partial x\partial\theta^2} + \frac{3}{2}\frac{\partial^2 V}{\partial x\partial\theta} - \frac{1}{2}R\frac{\partial^2 U}{\partial\theta^2}\right) = 0$$

$$L_2(U,V,W,p_{ij}) = \left(\frac{p_{21}}{R} + \frac{p_{51}}{R^2}\right)\frac{\partial^2 U}{\partial x\partial\theta} + \frac{1}{R}\left(\frac{p_{22}}{R} + \frac{p_{52}}{R^2}\right)\left(\frac{\partial^2 V}{\partial\theta^2} + \frac{\partial W}{\partial\theta}\right) - \left(\frac{p_{24}}{R} + \frac{p_{54}}{R^2}\right)\frac{\partial^3 W}{\partial x^2\partial\theta} + \frac{1}{R^2}\left(\frac{p_{25}}{R} + \frac{p_{52}}{R^2}\right)\left(-\frac{\partial^3 W}{\partial\theta^3} + \frac{\partial^2 V}{\partial\theta^2}\right) + \left(p_{33} + \frac{3p_{63}}{2R^2}\right)\left(\frac{\partial^2 V}{\partial x^2} + \frac{\partial^2 U}{R\partial x\partial\theta}\right) + \frac{1}{R}\left(p_{36} + \frac{3p_{66}}{2R}\right)\left(-2\frac{\partial^3 W}{\partial x^2\partial\theta} + \frac{3}{2}\frac{\partial^2 V}{\partial x^2} - \frac{\partial^2 U}{2R\partial x\partial\theta}\right) = 0$$

$$L_3(U,V,W,p_{ij}) = p_{41}\frac{\partial^3 U}{\partial x^3} + \frac{p_{42}}{R}\left(\frac{\partial^3 V}{\partial x^2\partial\theta} + \frac{\partial^2 W}{\partial x^2}\right) - p_{44}\frac{\partial^4 W}{\partial x^2} + \frac{p_{45}}{R^2}\left(-\frac{\partial^4 W}{\partial x^2\partial\theta^2} + \frac{\partial^3 V}{\partial x^2\partial\theta}\right) + \frac{2p_{63}}{R}\left(\frac{\partial^3 U}{R\partial x\partial\theta^2} + \frac{\partial^3 V}{\partial x^2\partial\theta}\right) + \frac{2p_{66}}{R^2}\left(-2\frac{\partial^4 W}{\partial x^2\partial\theta^2} + \frac{3}{2}\frac{\partial^3 V}{\partial x^2\partial\theta} - \frac{\partial^3 U}{2R\partial x\partial\theta^2}\right) + \frac{p_{51}}{R^2}\frac{\partial^3 U}{\partial x\partial\theta^2} + \frac{p_{52}}{R^2}\left(\frac{\partial^3 V}{\partial x\partial\theta^2} + \frac{\partial^2 W}{\partial\theta^2}\right) + \frac{p_{55}}{R^4}\left(\frac{\partial^4 W}{\partial\theta^4} + \frac{\partial^3 W}{\partial\theta^3}\right) - \frac{p_{21}}{R}\frac{\partial U}{\partial x} + \frac{p_{54}}{R}\frac{\partial^4 W}{\partial x^2\partial\theta^2} + \frac{p_{22}}{R^2}\left(\frac{\partial V}{\partial\theta} + W\right) + \frac{p_{24}}{R}\frac{\partial^2 W}{\partial\theta^2} - \frac{p_{25}}{R^3}\left(-\frac{\partial^2 W}{\partial\theta^2} + \frac{\partial V}{\partial\theta}\right) = 0$$

Elements of matrix $[H_{ij}]$

As mentioned above, A_j and B_j may be written in terms of C_j as follows:

$$A_j = \alpha_j C_j \text{ and } B_j = \beta_j C_j$$

The system of equations (4) may therefore be expressed by:

$$\begin{bmatrix} H_{11} & H_{12} \\ H_{21} & H_{22} \end{bmatrix}\begin{Bmatrix} \alpha_j \\ \beta_j \end{Bmatrix} = \begin{Bmatrix} -H_{13} \\ -H_{23} \end{Bmatrix}$$

To resolve the last system of equations, we need only the following coefficients:

$H_{11} = \lambda_j^2 - (1-\nu/2)n^2(1+k/4)$
$H_{12} = H_{21} = (n\lambda_j/2)(\nu(1+3k/4) + (1-3k/4))$
$H_{22} = -(1-\nu/2)\lambda_j^2 + n^2(1+k) - 9/8(1-\nu)\lambda_j^2$
$H_{13} = \nu\lambda_j - (1-\nu/2)k\lambda_j n^2$
$H_{23} = n(1+n^2k) - (3-\nu/2)kn\lambda_j^2$
Noting that : $H_{11}H_{22} - H_{21}H_{12} = -\left(\frac{1-\nu}{2}\right)(\lambda^2 - n^2)^2 \neq 0$
With: $k = (1/12)(t/R)^2$

Appendix B

Equations of motion for a thin multilayer anisotropic conical shell

$$S_1(U,V,W,B_{ij}) = B_{11}\left[2x\sin\alpha\frac{\partial U}{\partial x}+x^2\frac{\partial^2 U}{\partial x^2}\right]+B_{12}\left[x\frac{\partial^2 V}{\partial x\partial\theta}+x\cos\alpha\frac{\partial W}{\partial x}+U\sin\alpha+W\cos\alpha\right]-B_{14}\left[3x^2\sin\alpha\frac{\partial^2 W}{\partial x^2}+x^3\sin\alpha\frac{\partial^3 W}{\partial x^3}\right]$$
$$+B_{15}\left[x\cot\alpha\frac{\partial V}{\partial x\partial\theta}-\frac{x}{\sin\alpha}\frac{\partial^3 W}{\partial\theta^2\partial x}-2x\sin\alpha\frac{\partial W}{\partial x}-x^2\sin\alpha\frac{\partial^2 W}{\partial x^2}+\cot\alpha\frac{\partial V}{\partial\theta}-\frac{1}{\sin\alpha}\frac{\partial^2 W}{\partial\theta^2}\right]+B_{24}\left[x^2\sin\alpha\frac{\partial^2 W}{\partial x^2}\right]$$
$$-B_{22}\left[\frac{\partial V}{\partial\theta}+\sin\alpha U+\cos\alpha W\right]+B_{25}\left[-\cot\alpha\frac{\partial V}{\partial\theta}+\frac{1}{\sin\alpha}\frac{\partial^2 W}{\partial\theta^2}+x\sin\alpha\frac{\partial W}{\partial x}\right]+B_{33}\left[x\frac{\partial^2 V}{\partial x\partial\theta}+\frac{1}{\sin\alpha}\frac{\partial^2 U}{\partial\theta^2}-\frac{\partial V}{\partial\theta}\right]$$
$$+B_{36}\left[-\frac{2x}{\sin\alpha}\frac{\partial^3 W}{\partial\theta^2\partial x}+x\cot\alpha\frac{\partial^2 V}{\partial x\partial\theta}-\frac{\cot\alpha}{\sin\alpha}\frac{\partial^2 U}{\partial\theta^2}+\frac{2}{\sin\alpha}\frac{\partial^2 W}{\partial\theta^2}-\cot\alpha\frac{\partial V}{\partial\theta}\right]$$
$$+B_{66}\left[\frac{x\cot\alpha}{\sin\alpha}\frac{\partial^3 W}{\partial\theta^2\partial x}-\frac{3x}{4}\cot^2\alpha\frac{\partial^2 V}{\partial x\partial\theta}+\frac{\cot^2\alpha}{4\sin\alpha}\frac{\partial^2 U}{\partial\theta^2}-\frac{\cot\alpha}{\sin\alpha}\frac{\partial^2 W}{\partial\theta^2}+\frac{3\cot^2\alpha}{4}\frac{\partial V}{\partial\theta}\right]$$

$$S_2(U,V,W,B_{ij}) = B_{12}x\frac{\partial^2 U}{\partial x\partial\theta}+B_{15}x\cot\alpha\frac{\partial^2 U}{\partial x\partial\theta}+B_{22}\left[\frac{1}{\sin\alpha}\frac{\partial^2 V}{\partial\theta^2}+\frac{\partial U}{\partial\theta}+\cot\alpha\frac{\partial W}{\partial\theta}\right]-B_{24}x^2\frac{\partial^3 W}{\partial x^2\partial\theta}-B_{45}x^2\cot\alpha\frac{\partial^3 W}{\partial x^2\partial\theta}$$
$$+B_{25}\left[\frac{2\cot\alpha}{\sin\alpha}\frac{\partial^2 V}{\partial\theta^2}-\frac{1}{\sin^2\alpha}\frac{\partial^3 W}{\partial\theta^3}-x\frac{\partial^2 W}{\partial x\partial\theta}+\cot^2\alpha\frac{\partial W}{\partial\theta}+\cot\alpha\frac{\partial U}{\partial\theta}\right]+B_{55}\left[\frac{\cot^2\alpha}{\sin\alpha}\frac{\partial^2 V}{\partial\theta^2}-\frac{\cot\alpha}{\sin^2\alpha}\frac{\partial^3 W}{\partial\theta^3}-x\cot\frac{\partial^2 W}{\partial x\partial\theta}\right]$$
$$+B_{33}\left[x^2\sin\alpha\frac{\partial^2 V}{\partial x^2}+x\cot\alpha\frac{\partial^2 U}{\partial x\partial\theta}-4x\frac{\partial^2 W}{\partial x\partial\theta}+6x\cos\alpha\frac{\partial V}{\partial x}+2\cot\alpha\frac{\partial U}{\partial\theta}+4\frac{\partial W}{\partial\theta}-6\cos\alpha V\right]$$
$$+B_{66}\left[-6x\cot\alpha\frac{\partial^2 W}{\partial x\partial\theta}-3x^2\cot\alpha\frac{\partial^3 W}{\partial x^2\partial\theta}+\frac{9x}{2}\cos\alpha\cot\alpha\frac{\partial V}{\partial x}+\frac{9x^2}{4}\cos\alpha\cot\alpha\frac{\partial^2 V}{\partial x^2}-\frac{3}{2}\cot^2\alpha\frac{\partial U}{\partial\theta}\right.$$
$$\left.-\frac{3x}{4}\cot^2\alpha\frac{\partial^2 U}{\partial x\partial\theta}+6\cot\alpha\frac{\partial W}{\partial\theta}-\frac{9}{2}\cos\alpha\cot\alpha V\right]$$

$$S_3(U,V,W,B_{ij}) = -B_{12}x\cos\alpha\frac{\partial U}{\partial x}+B_{14}\left[6x\sin\alpha\frac{\partial U}{\partial x}+6x^2\sin\alpha\frac{\partial^2 U}{\partial x^2}+x^3\sin\alpha\frac{\partial^3 U}{\partial x^3}\right]+B_{15}\left[\frac{x}{\sin\alpha}\frac{\partial^3 U}{\partial\theta^2\partial x}-2x\sin\alpha\frac{\partial U}{\partial x}-x^2\sin\alpha\frac{\partial^2 U}{\partial x^2}\right]$$
$$+B_{24}\left[4x\frac{\partial^2 V}{\partial x\partial\theta}+x^2\frac{\partial^3 V}{\partial x^2\partial\theta}+4x\sin\alpha\frac{\partial U}{\partial x}+x^2\sin\alpha\frac{\partial^2 U}{\partial x^2}+4x\cos\alpha\frac{\partial W}{\partial x}+2x^2\cos\alpha\frac{\partial^2 W}{\partial x^2}+2\frac{\partial V}{\partial\theta}+2\sin\alpha U+2\cos\alpha W\right]$$
$$+B_{25}\left[-\cot^2\alpha\frac{\partial V}{\partial\theta}+\frac{1}{\sin^2\alpha}\frac{\partial^3 V}{\partial\theta^3}+\frac{1}{\sin\alpha}\frac{\partial^2 U}{\partial\theta^2}+2\frac{\cot\alpha}{\sin\alpha}\frac{\partial^2 W}{\partial\theta^2}-\frac{\partial V}{\partial\theta}-x\frac{\partial^2 V}{\partial x\partial\theta}-\sin\alpha U-x\sin\alpha\frac{\partial U}{\partial x}-\cos\alpha W\right]$$
$$+B_{36}\left[6x\frac{\partial^2 V}{\partial x\partial\theta}+2x^2\frac{\partial^3 V}{\partial x^2\partial\theta}+\frac{4}{\sin\alpha}\frac{\partial^2 U}{\partial\theta^2}+\frac{2x}{\sin\alpha}\frac{\partial^3 U}{\partial\theta^2\partial x}-4\frac{\partial V}{\partial\theta}-2x\frac{\partial^2 V}{\partial x\partial\theta}\right]$$

Elements of matrix $[D_{ij}]$

$$[D]=\begin{bmatrix} A\lambda^2+C & R\lambda+T & F\lambda^3+G\lambda^2+H\lambda+J \\ -R\lambda+T & Y\lambda^2+L & M\lambda^2+N\lambda+P \\ -F\lambda^3+G\lambda^2-H\lambda+J & M\lambda^2-N\lambda+P & Q\lambda^4+S\lambda^2+Z \end{bmatrix}$$

where:

$$A = B_{11}\sin\alpha/4$$

$$C = B_{12}\sin\alpha + n^2B_{36}\cot\alpha/\sin\alpha - n^2B_{33}/\sin\alpha - B_{22}\sin\alpha - n^2B_{66}(\cot\alpha)^2/(4\sin\alpha)$$
$$-B_{11}\sin\alpha/4$$

$$R = nB_{12}/2 + nB_{15}\cot\alpha/2 + nB_{33}/2 + nB_{36}\cot\alpha/2 - 3nB_{66}(\cot\alpha)^2/8$$

$$T = nB_{12}/2 + nB_{15}\cot\alpha/2 - nB_{22} - nB_{25}\cot\alpha - 3nB_{33}/2 - 3nB_{36}\cot\alpha/2 + 9nB_{66}(\cot\alpha)^2/8$$

$$F = -B_{41}\sin\alpha/8$$

$$G = 3B_{41}\sin\alpha/8 - B_{51}\sin\alpha/4 + B_{42}\sin\alpha/4$$

$$H = B_{21}\cos\alpha/2 + n^2 B_{51}/(2\sin\alpha) + n^2 B_{63}/\sin(\alpha) + B_{52}\sin\alpha/2 - n^2 B_{66}\cot\alpha/(2\sin\alpha) - B_{42}\sin\alpha + B_{41}(\sin\alpha)/8$$

$$J = B_{12}\cos\alpha/2 + n^2 B_{51}/(2\sin\alpha) + B_{51}\sin\alpha/4 - B_{22}\cos\alpha - n^2 B_{52}/\sin\alpha - B_{52}\sin\alpha/2 - 3B_{41}\sin\alpha/8 + 3B_{42}\sin\alpha/4 - 3n^2 B_{63}/\sin\alpha + 3n^2 B_{66}\cot\alpha/(2\sin\alpha)$$

$$Y = B_{33}\sin\alpha/4 + 3B_{36}\sin\alpha/4 + 9B_{66}(\cos\alpha\cot\alpha)/16$$

$$L = -9B_{33}\sin\alpha/4 - 27B_{36}\cos\alpha/4 - 81B_{66}\cos\alpha\cot\alpha/16 - 2n^2 B_{52}\cot\alpha/\sin\alpha - n^2 B_{55}(\cot\alpha)^2/\sin\alpha - n^2 B_{22}/\sin\alpha$$

$$M = nB_{24}/4 + nB_{36}/2 + nB_{54}\cot\alpha/4 + 3nB_{66}\cot\alpha/4$$

$$N = -nB_{24} + nB_{25}/2 - nB_{54}\cot\alpha + nB_{55}\cot\alpha/2$$

$$P = -nB_{22}\cot\alpha - n^3 B_{25}/(\sin\alpha)^2 - nB_{25}/2 - nB_{52}(\cot\alpha)^2 + 3nB_{24}/4 - 9nB_{36}/2 + 3nB_{54}\cot\alpha/4 - n^3 B_{55}\cot(\alpha)/(\sin\alpha)^2 - nB_{55}\cot\alpha/2 - 27nB_{66}\cot\alpha/4$$

$$Q = -B_{44}\sin\alpha/16$$

$$S = B_{42}\cos\alpha/2 - 3B_{45}\sin\alpha/4 + n^2 B_{66}/\sin\alpha + n^2 B_{54}/\sin\alpha + B_{55}\sin\alpha/4 + 5B_{44}\sin\alpha/8$$

$$Z = -9n^2 B_{66}/\sin\alpha - 2n^2 B_{25}\cot\alpha/\sin\alpha - n^2 B_{55}/\sin\alpha - n^4 B_{55}/(\sin\alpha)^3 - B_{55}\sin\alpha/4 - B_{22}\cos\alpha\cot\alpha + 3B_{42}\cos\alpha/2 + 3n^2 B_{54}/(2\sin\alpha) - 9B_{44}\sin\alpha/16 + 3B_{45}\sin\alpha/4 - B_{25}\cos\alpha$$

where:

B_{ij} coefficients are given in reference [6].

Appendix C: List of Symbols

U, V, and W	axial, circumferential and radial displacements, respectively
A, B, and C	constants in equations defining *U, V, W,* respectively
l_e	finite element length
a, b, c and d	coefficients of characteristic equation (5)
n	circumferential mode number
K	bending stiffness, $Et^3/(12(1-\nu^2)$
D	membrane stiffness, $Et/(1-\nu^2)$
E	Young's modulus
t	thickness of shell
R_e	mean radius of the axisymmetric finite element
J_n	Bessel function of the first kind of order n
Y_n	Bessel function of the second kind of order n
λ_j *(j =1-8)*	complex roots of the characteristic equation
V_x, V_θ *and* V_r	axial, tangential and radial components of the fluid velocity, respectively
i	complex number, i^2=-1
x, r and θ	axial, radial and circumferential coordinates
v	Poisson's ratio
ρ_s	density of shell
ρ_f	density of fluid
B_{ij}	components of an anisotropic matrix of elasticity for conical shell
δ	thickness proportionality coefficient
ϕ	velocity potential function
ω	natural frequency (rad/s)
β	Coordinate along the semi vertex angle
$[P]$	elasticity matrix
$[N]$	shape functions matrix
$[R]$	matrix of order 3×8 defined in equation (7)
$[D]$	matrix of order 3×3 defined in equation (23)
$\{\delta\}^e$	nodal displacement vector
$\{\varepsilon\}$	Strain vector
$[Q]$	matrix of order 6×8 given in equation (12)
$\{\sigma\}$	resultant stress vector
$[B]$	matrix of order 6×8 given in equation (12)
$[m_s]^e$	elementary mass matrix of order 8×8
$[k_s]^e$	elementary stiffness matrix of order 8×8
$\{F\}^e$	elementary load vector
$\{P\}$	vector expressing the pressure applied by the fluid
$[R_f]$	matrix of order 3×8 that contains only the second line of matrix $[R]$
$[A_f]^{-1}$	matrix of order 8×8 defined in equation (49)
$[S_f]$	matrix defined in equation (50)
$[m_f]$	added mass matrix of order 8×8
$[T]$	geometrical transformation matrix of order 4×4
$[T_f]$	transformation matrix of fluid added mass of order 4×4
$[M_s]$	global mass matrix
$[K_s]$	global stiffness matrix
$[M_f]$	global fluid added mass
$\{\delta_g\}$	global displacement vector